



**CHALMERS**  
UNIVERSITY OF TECHNOLOGY

## **Design and Fabrication of Flexible Copper Sensor Decorated with Bismuth Micro/Nanodendrites to Detect Lead and Cadmium in Noninvasive Samples**

Downloaded from: <https://research.chalmers.se>, 2024-04-25 14:32 UTC

Citation for the original published paper (version of record):

de Campos, A., Rosa Da Silva, R., Calegari, M. et al (2022). Design and Fabrication of Flexible Copper Sensor Decorated with Bismuth Micro/Nanodendrites to Detect Lead and Cadmium in Noninvasive Samples of Sweat. *Chemosensors*, 10(11).  
<http://dx.doi.org/10.3390/chemosensors10110446>

N.B. When citing this work, cite the original published paper.

## Article

# Design and Fabrication of Flexible Copper Sensor Decorated with Bismuth Micro/Nanodendrites to Detect Lead and Cadmium in Noninvasive Samples of Sweat

Anderson M. de Campos<sup>1</sup>, Robson R. Silva<sup>2</sup>, Marcelo L. Calegari<sup>3</sup>  and Paulo A. Raymundo-Pereira<sup>4,\*</sup>

<sup>1</sup> Chair of Physical Chemistry, Department of Chemistry, University of Munich (LMU), Butenandstr. 5-13, 81377 Munich, Germany

<sup>2</sup> Department of Chemistry and Chemical Engineering, Chalmers University of Technology, SE-412 96 Gothenburg, Sweden

<sup>3</sup> São Carlos Institute of Chemistry, University of São Paulo, São Carlos 13566-590, Brazil

<sup>4</sup> São Carlos Institute of Physics, University of São Paulo (USP), São Carlos 13566-590, Brazil

\* Correspondence: pauloaugustoraymundopereira@gmail.com

**Abstract:** The use of economic methods to design and fabricate flexible copper sensors decorated with bismuth micro/nanodendrites for the detection of lead and cadmium in sweat is demonstrated. The flexible copper sensors were constructed with simple and cost-effective materials; namely, flexible and adhesive conductive copper tape, adhesive label containing the design of a three-electrode electrochemical system, and nail polish or spray as a protective layer. The flexible copper device consisted of a working electrode decorated with bismuth micro/nanodendrites using an electrodeposition technique, a copper pseudo-reference and copper counter electrodes. Under optimal experimental conditions, the flexible sensing platform showed excellent performance toward the detection of lead and cadmium using differential pulse anodic stripping voltammetry (DPAdSV) in a wide linear range from 2.0  $\mu\text{M}$  to 50  $\mu\text{M}$  with acceptable reproducibility and repeatability, and limits of detection and quantification of 5.36 and 17.9  $\mu\text{M}$  for  $\text{Cd}^{2+}$  ions and 0.76  $\mu\text{M}$  and 2.5 for  $\text{Pb}^{2+}$  ions. Studies of addition and recovery in spiked artificial sweat sample were performed, with a recovery of 104.6%. The flexible copper device provides a great opportunity for application in wearable perspiration-based healthcare systems or portable sensors to detect toxic metals in biological samples.

**Keywords:** flexible sensor; copper tape; bismuth micro/nanostructures; lead; cadmium; electrochemical detection; sweat



**Citation:** de Campos, A.M.; Silva, R.R.; Calegari, M.L.; Raymundo-Pereira, P.A. Design and Fabrication of Flexible Copper Sensor Decorated with Bismuth Micro/Nanodendrites to Detect Lead and Cadmium in Noninvasive Samples of Sweat. *Chemosensors* **2022**, *10*, 446. <https://doi.org/10.3390/chemosensors10110446>

Academic Editors: Song Gao, Yang Li and Wenjing Yue

Received: 9 September 2022

Accepted: 24 October 2022

Published: 27 October 2022

**Publisher's Note:** MDPI stays neutral with regard to jurisdictional claims in published maps and institutional affiliations.



**Copyright:** © 2022 by the authors. Licensee MDPI, Basel, Switzerland. This article is an open access article distributed under the terms and conditions of the Creative Commons Attribution (CC BY) license (<https://creativecommons.org/licenses/by/4.0/>).

## 1. Introduction

Human body fluids such as saliva, urine, blood, tears, interstitial fluid (IF), and sweat are constituted of electrolytes, hormones, metabolites, salts, and proteins, which are used to noninvasively monitor health conditions of individuals [1–3]. Sweat has been extensively used due to ease of sampling, simplicity of operation and obtainment, and the extensive interface of the skin [3]. Several heavy metals can be present in human perspiration, including Zn, Pb, Cu, Cd, Mg, Ni, Ca, Hg, Na, and K ions, and are closely related to human health conditions [4–7]. Lead ( $\text{Pb}^{2+}$ ) and cadmium ( $\text{Cd}^{2+}$ ) show toxic effects on the systems of human body, including the endocrine, nervous, circulatory, immunological, digestive, and cardiovascular systems [8], due to the accumulation characteristic in tissues; the respiratory system is the main route of intoxication with heavy metals [9]. Exposure to the high levels of cadmium cause inflammatory responses and destructive problems in the respiratory tract, kidney, liver [9]; for example, Fanconi syndrome is associated with severe bone pain [10]. Lead intoxication causes damage to the brain and central nervous system, increased behavioral disorders, irritability, fatigue, intellectual disability, learning difficulties, anemia, infertility, increase in blood pressure, renal impairment and development of chronic kidney

disease, decline in mental functioning and cognitive impairment, loss of appetite, and in some cases leads to coma, seizures, and even death [8,10,11]. Therefore, the monitoring of  $Pb^{2+}$  and  $Cd^{2+}$  exposure using human body fluids can provide insight into human health status and inform auxiliary therapeutic and toxicological studies.

Gold standard techniques to detect heavy metals in human biological fluids use unportable and expensive analytical instruments, including inductively coupled plasma mass spectrometry (ICP-MS) [12] and atomic absorption spectroscopy (AAS) [13], making them difficult to use for on-site detection and continuous monitoring. As an alternative, sensors play a decisive role in transferring biosensing technologies to portable meters for tracking hazardous compounds in decentralized analysis, reflecting advantages such as speed, miniaturization, scalability, low power requirements, and low cost [14]. Moreover, electrochemical devices can be combined with preconcentration or deposition steps, accumulating heavy metals at the working electrode surface, making anodic stripping analysis the most sensitive and effective electroanalytical technique [8]. The most commonly used electrode materials as nonflexible supports are gold [15], carbon paste [16], glassy carbon [17,18], and indium tin oxide [19,20]; however, they are rarely applied in the monitoring of heavy metals in a portable system [21]. The flexible sensing systems are generated by photolithography [22,23], direct laser writing [24], inkjet printing [25], e-beam evaporation [26], wax printing [27], soft lithography [28], plasma etching [29], and electrodeposition [30] techniques. However, most of these methods require fabrication processes with sophisticated and expensive instruments, time-consuming steps, and in some cases, need a clean work space [21]. Wei gao et. al. reported a microsensor array designed to simultaneously detect multiple heavy metals, including Zn, Cd, Pb, Cu, and Hg, using square wave anodic stripping voltammetry (SWASV), in which a microchip array was constructed on a flexible polyethylene terephthalate (PET) substrate in a protocol involving multiple steps of photolithography, evaporation (Cr/Au, Ag, Bi), and lift off [8]. Alternatively to the exhaustive and expensive protocols, Xig Xuan et. al. reported a flexible graphene-based electrode formed by laser-writing and substrate-transfer techniques for zinc detection in sweat [4]. Due to the toxicity of lead and cadmium and the importance of management, the design and fabrication of flexible sensors using facile, inexpensive, and rapid prototyping methods to produce at a large scale is fundamental for on-site management of individual health states [8,21].

Bismuth-based electrodes have been selected because they are an environmentally friendly alternative to mercury electrodes due to their low toxicity, and their ability to form amalgam (metal alloys) with toxic metals [4,8,31]. The development and use of greener electrode materials is extremely attractive for the routine use of disposable (“one-shot”) metal sensors [31]. Bismuth electrodes display a well-defined, undistorted, and highly reproducible stripping response, exhibiting excellent resolution of neighboring peaks, wide linear dynamic range, with signal-to-background characteristics comparable to those of common mercury electrodes [4,8,31]. While amalgam formation is responsible for the stripping performance of mercury electrodes, the attractive and unique behavior of bismuth film electrodes is attributed to the formation of multicomponent alloys [31]. Bismuth-based electrodes are known to form binary- or multicomponent “fusible” alloys with numerous heavy metals using stripping analysis of elements with standard potentials more negative than bismuth (i.e., Zn, Ga, Cd, In, Tl, Sn, Pb) [31]. The attractive behavior of the “mercury-free” flexible copper sensors, associated with the negligible toxicity of bismuth, hold great promise for “one-shot” decentralized metal detecting. Moreover, Bi micro/nanostructures are a great material for working electrodes, offering biocompatibility, high sensitivity, and wide operational potential range owing to their stability and low influence of dissolved oxygen [8,31]. In this work, we designed a flexible copper electrochemical sensor with an easy, inexpensive, and prototyping method to detect lead and cadmium in sweat samples. The flexible sensory platform contains a full electrochemical system with an auxiliary (AE) and reference (RE) electrode consisting of copper tape, and a working (WE)

electrode consisting of copper tape decorated with bismuth micro/nanodendrites obtained via electrodeposition.

## 2. Materials and Methods

### 2.1. Reagents and Solutions

Bismuth(III) nitrate pentahydrate (99%), sodium acetate (99%), acetic acid (95%), lead(II) nitrate (99%), cadmium(II) nitrate (99%), lactic acid (95%), urea (98%), sodium chloride (99%), and potassium chloride (99%) were purchased from Sigma-Aldrich (St. Louis, MO, USA). Hydrochloric acid and sodium citrate were acquired from Synth. All other reagents were of analytical grade and used as received. Ferric chloride solution (iron(III) chloride solution) was purchased from Suetoku. All solutions were prepared with ultrapure water (resistivity > 18.0 M $\Omega$  cm) obtained from a Millipore Milli-Q system (Billerica, MA, USA).

### 2.2. Instruments

Electrochemical measurements were performed using a PGSTAT204 Autolab (Eco Chemie, Utrecht, The Netherlands) potentiostat/galvanostat controlled by NOVA software, 2.0 version. Electron microscopy images of bismuth micro/nanodendrites were obtained with a Zeiss Sigma (Zeiss, Oberkochen, Germany) scanning electron microscope equipped with a field emission electron gun (SEM-FEG) operating at 20 kV and OXFORD qualitative and quantitative chemical analysis system. The Raman spectra were measured with a micro-Raman spectrometer (LabRAM Horiba Jobin Yvon-model HR 800), equipped with a He-Ne laser at 632.81 nm (17 mW) and a CCD camera. The measurements were performed in backscattering configuration with 50 $\times$  WD objective (Olympus MPL) by exposing the samples during 30 s of acquisition for three accumulation intervals. The slit width of the Raman spectrometer was 100  $\mu$ m, and a diffraction grating of 600 lines/mm was used. X-ray powder diffraction (XRD) was acquired with a D8 Advance X-ray diffractometer (Bruker) operated at 40 mA and 40 kV, employing Ni-filtered Cu K $\alpha$  X-ray radiation ( $\lambda$  = 1.540 Å).

### 2.3. Preparation of Sweat Samples

Analyses of cadmium and lead ions in synthetic sweat samples were prepared as reported by Mathew et al. [32], consisting of 1.0 g·L<sup>-1</sup> of urea, 1.0 g·L<sup>-1</sup> of KCl, 7.5 g·L<sup>-1</sup> of NaCl, and 1.0 mL·L<sup>-1</sup> of lactic acid solubilized in 0.1 mol·L<sup>-1</sup> of acetate buffer solution.

## 3. Results

### 3.1. Design and Fabrication of Flexible Copper Sensor Decorated with Bismuth Micro/Nanodendrites

The flexible copper sensors decorated with bismuth micro/nanodendrites were fabricated on a flexible polyethylene terephthalate (PET) substrate using a procedure with simple steps and inexpensive materials, as demonstrated in Figure 1. A flexible, conductive copper adhesive tape (thickness of 40  $\mu$ m) was cut in pieces of 5  $\times$  4 cm (Figure 1(Ai)) and glued onto PET, as depicted in Figure 1(Aii). Copper surfaces were cleaned with paper towels and acetone. A template containing the design of electrochemical devices was generated on an adhesive label sheet (Pimaco<sup>®</sup>) with a Silhouette Cameo model 3 cutting machine, and glued onto the copper adhesive tape, as shown in Figure 1(Aiii). The rectangular shape of electrodes was chosen to facilitate the Silhouette Cameo cutting machine work. The entire surface was covered with a polymer layer using nail polish (Figure 1(Aiv,Av)), transferring the design of the devices contained in the template for the copper adhesive surface after removing the mask, as can be seen in Figure 1(Avi). The exposed copper was removed by a corrosion step through the immersion of devices in inexpensive concentrated ferric chloride solution for 20 min, followed by a wash step with distilled water (Figure 1(Avii)). The corrosion step should be not too long to avoid the side erosion phenomenon, which can affect the area of working electrodes. The polymer layer was removed with acetone-soaked paper towels and then the flexible copper sensors were ready to use, as shown in Figure 1(Aviii).

The procedure described here is generic, and can be used for others metallic surface, e.g., gold and nickel, alternatively to the expensive photolithography process. Figure 1(Bi) depicts a detailed representation of a flexible copper sensor with a complete electrochemical system containing auxiliary (AE), pseudo-reference (RE), and working electrodes (WE). An insulation tape (Scotch, 3M) of flexible polyvinyl chloride (PVC) was used to delimit the area of the working electrodes. Figure 1(Bii) depicts the working electrode decorated with bismuth micro/nanodendrites electrochemically deposited in a solution containing  $0.02 \text{ mol}\cdot\text{L}^{-1}$  of bismuth(III) nitrate,  $1.0 \text{ mol}\cdot\text{L}^{-1}$  of hydrochloric acid, and  $0.15 \text{ mol}\cdot\text{L}^{-1}$  of sodium citrate at a constant potential of  $-0.18 \text{ V}$  (vs. Ag/AgCl) for 60 s [33]. The layer of micro/nanodendrites was selectively deposited on the working electrode using the electrodeposition technique, in which the WE are polarized cathodically, reducing the bismuth ions on the copper surface. The formation of bismuth micro/nanodendrites is controlled by the applied potential and time of the applied potential. Different applied potential will produce structures without specific morphology, and the time will control the amount of electrodeposited bismuth. The flexible copper sensor can be connected to a potentiostat using any commercial or lab-built connector for screen-printed electrodes, e.g., DropSens connectors ref. CAC4MMH or DSC4MM. Figure 1(Biii) shows a schematic representation of the preconcentration step of lead and cadmium analysis of a sweat sample.

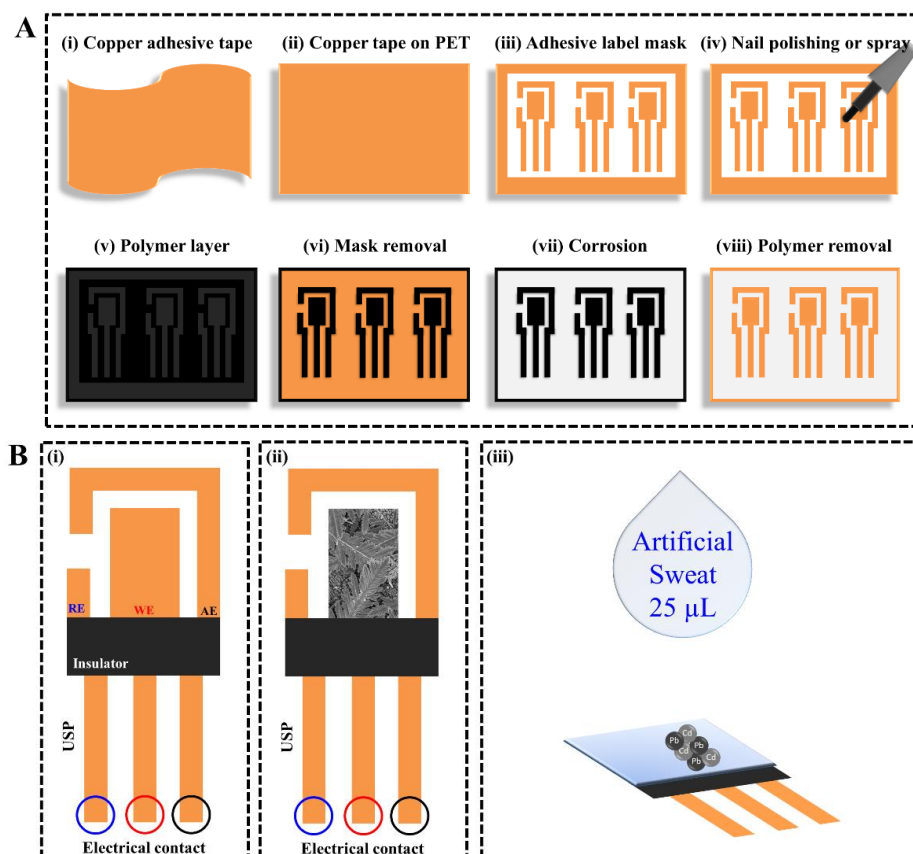


**Figure 1.** Schematic representation of the design and fabrication of a flexible copper sensor decorated with bismuth micro/nanodendrites. (A): (i) conductive copper adhesive tape; (ii) copper adhesive tape glued onto PET substrate; (iii) adhesive tape mask glued onto copper; (iv) the surface is painted with nail polish or spray; (v) a polymer layer covered the surface; (vi) the adhesive tape mask is removed from the surface; (vii) the copper is corroded; (viii) the polymer layer is removed with acetone and then the flexible copper sensors are ready to use. (B): (i) Detailed representation of flexible copper sensor with a complete electrochemical system containing auxiliary (AE), pseudo-reference (RE), and working electrodes (WE); (ii) working electrode decorated with bismuth micro/nanodendrites; (iii) analysis of lead and cadmium in artificial sweat sample. USP refers to the University of Sao Paulo.

The structural morphology of bismuth micro/nanodendrites was inspired by rime ice from cold areas, as illustrated in Figure 2A,B. The conductive flexible copper substrate acts as a tree branch because the bismuth micro/nanodendrites are grown electrochemically similarly to the ice. Initially, the bismuth structures seeds onto the flexible copper surface, and they are continuously electrodeposited on the seed producing rime-ice-like micro/nanostructures, as depicted in Figure 2A,B. Figure 2C depicts the Raman spectra containing five peaks located at 64, 93, 124, 308, and 464  $\text{cm}^{-1}$  of the bismuth micro/nanodendrites deposited on flexible copper sensor. The two peaks at 66 and 92  $\text{cm}^{-1}$  are indicative of the rhombohedral bismuth structure [34]. The three weak Raman peaks centered at 124, 308, and 464  $\text{cm}^{-1}$  are attributed to the  $\beta\text{-Bi}_2\text{O}_3$  (tetragonal) phase [34,35]. No significant change in the bare flexible copper sensor and flexible copper sensor decorated with bismuth micro/nanodendrites after  $\text{Pb}^{2+}$  and  $\text{Cd}^{2+}$  ion sensing was detected by EDS or XRD, as depicted in Figure 2D,E, indicating that there was no corrosion after the sensing step. This high catalytic stability is therefore attributed to the physical and chemical stability of bismuth micro/nanodendrites. The XRD pattern of the flexible copper sensor decorated with bismuth micro/nanodendrites (top, in gray) shows six diffraction peaks at  $22.7^\circ$ ,  $26.5^\circ$ ,  $27^\circ$ ,  $37.8^\circ$ ,  $39.7^\circ$ ,  $47.3^\circ$ , and  $48.7^\circ$  attributed to the (003), (111), (012), (104), (110), (024), (116), and (112) planes of  $\text{Bi}_2\text{O}_3$  [PDF#41-1449] [36]. The XRD pattern of bare flexible copper sensor (bottom, in orange) depicts three diffraction peaks at  $43^\circ$ ,  $50.5^\circ$ , and  $74.3^\circ$  attributed to the (111), (200), and (220) planes of the FCC copper phase [JCPDS# 65-9026] [21]. The flexible copper sensor was successfully decorated with bismuth micro/nanodendrites using an easy preparation process with which it is also quite simple and efficient to detect  $\text{Cd}^{2+}$  and  $\text{Pb}^{2+}$  in sweat.

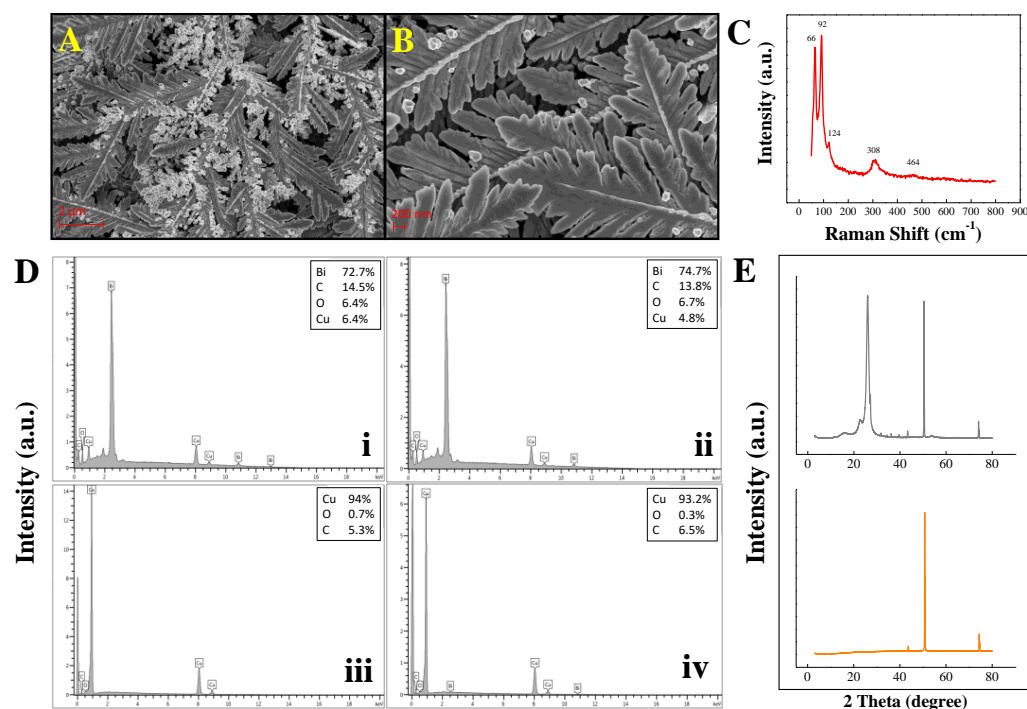


**Figure 2.** SEM-FEG image for flexible copper sensor decorated with bismuth micro/nanodendrites under different magnifications of 20,000 $\times$  in (A) and 50,000 $\times$  in (B). Raman spectra of flexible copper sensor decorated with bismuth micro/nanodendrites in (C). Energy-dispersive X-ray spectroscopy for flexible copper sensor decorated with bismuth micro/nanodendrites before (D(i)) and after (D(ii)) sensing, and for bare flexible copper sensor before (D(iii)) and after (D(iv)) sensing. XRD patterns of flexible copper sensor decorated with bismuth micro/nanodendrites (top, in gray) and bare flexible copper sensor (bottom, in orange) in (E).

### 3.2. Analytical Performance

Bismuth is a promising electrode material for lead, cadmium, and zinc detection; however, it is not appropriate for the anodic stripping of copper and mercury ions due to its lower oxidation potential ( $\sim -0.2$  V). Hence, a flexible copper sensor decorated with bismuth micro/nanodendrites can only be used for cadmium and lead detection, because zinc can react with chloride ions from sweat, forming chloro complexes with different oxidation states, leading to competition with cadmium and lead ions. Taking into account that the focus of this work is to demonstrate the design and fabrication of flexible copper sensor decorated with bismuth micro/nanodendrites, the deposition potential and deposition time were strategically chosen to be  $-1.0$  V, due to the fact that zinc ions can interfere, for which the oxidation peak is centered between  $-1.4$  V and  $-1.0$  V; they can also form chloride complexes with different oxidation state, and due to strong hydrogen evolution [4,8]. Similarly to the zinc ions, the copper ions were not selected because the reoxidation of  $\text{Cu}^{2+}$  can occur in the potential range between  $-0.2$  V and  $0.2$  V (vs. Bi), in which the copper from the electrode can be oxidized, decreasing the accuracy of the analysis. The deposition time was 60 s, indicating a rapid method using devices fabricated with low-cost materials. Figure 3A depicts voltammograms (DPASV) with two distinct oxidation peaks at  $-0.5$  V and  $-0.35$  V for simultaneous detection of cadmium and lead in artificial sweat obtained in the concentration ranges between  $2.0$  and  $50$   $\mu\text{M}$  for  $\text{Pb}^{2+}$  and  $0.5$  and  $10$   $\mu\text{M}$  for  $\text{Cd}^{2+}$ . The metallic ions in solution are reduced on the flexible copper sensor decorated with a bismuth micro/nanodendrites surface ( $\text{M}^{+n} + n\text{e}^- \rightarrow \text{M}(\text{Bi})$ ) followed by reoxidation initiated with anodic stripping. The anodic peak potential was shifted due to copper reference electrode, which can be addressed using silver ink. The anodic current peak increased linearly with the concentration in agreement with DPASV, as demonstrated in Figure 3A. The equations of linear regression of the analytical curves shown in Figure 3B,C are:  $I$  (A) =  $2.6 \times 10^{-7} + 1.0 C_{\text{cadmium}}$  ( $\text{mol}\cdot\text{L}^{-1}$ ) with  $r = 0.997$  and  $I$  (A) =  $-1.8 \times 10^{-5} + 6.4 C_{\text{lead}}$  ( $\text{mol}\cdot\text{L}^{-1}$ ) with  $r = 0.995$ . The detection limits were  $5.36$   $\mu\text{M}$  for  $\text{Cd}^{2+}$  and  $0.76$   $\mu\text{M}$  for  $\text{Pb}^{2+}$ .

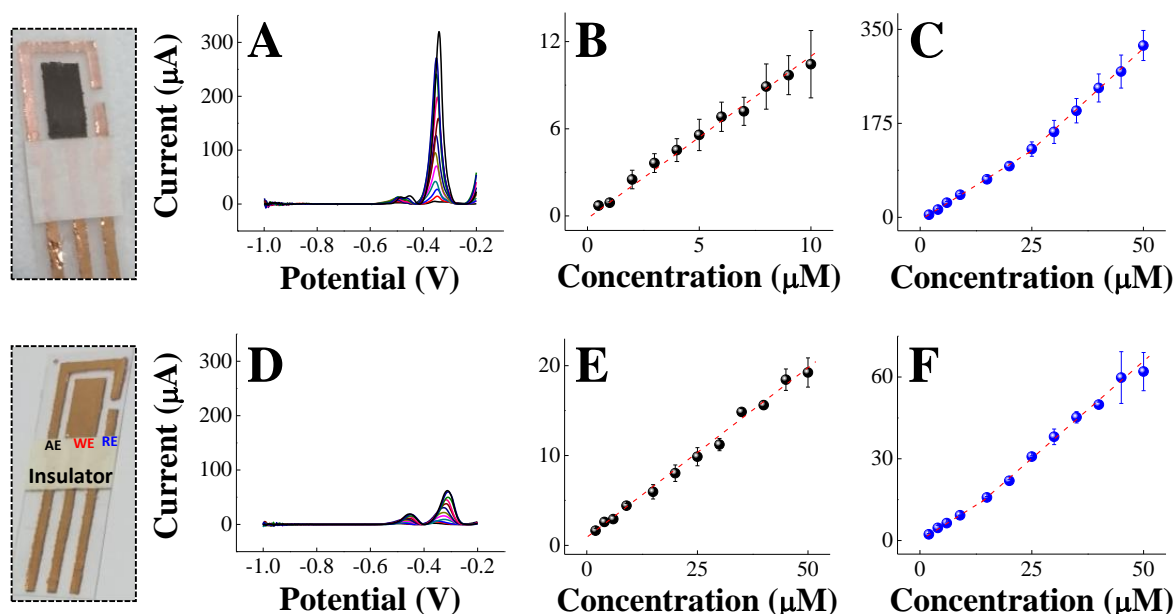


**Figure 3.** Differential pulse anodic stripping voltammetry in (A) and analytical curves for  $\text{Cd}^{2+}$  in (B) and  $\text{Pb}^{2+}$  in (C) obtained for flexible copper sensors decorated with bismuth micro/nanodendrites. Differential pulse anodic stripping voltammetry in (D) and analytical curves for  $\text{Cd}^{2+}$  in (E) and  $\text{Pb}^{2+}$  in (F) obtained for bare flexible copper sensor. Conditions: simultaneous detection of heavy metals with the concentration varying from  $2.0$   $\mu\text{M}$  to  $50$   $\mu\text{M}$  in artificial sweat.

The simultaneous detection of cadmium and lead was also performed with bare flexible copper sensors, as shown in Figure 3D. All DPAS voltammograms were well-defined with well-separated oxidation peaks and a narrow linear concentration range from 2 to 50  $\mu\text{M}$ . The current signals at  $-0.45\text{ V}$  and  $-0.30\text{ V}$  generated analytical curves with linear regressions of  $I\text{ (A)} = -7.4 \times 10^{-7} + 0.4 C_{\text{cadmium}}\text{ (mol}\cdot\text{L}^{-1})$ ,  $r = 0.999$ , and  $I\text{ (A)} = -1.8 \times 10^{-6} + 1.3 C_{\text{lead}}\text{ (mol}\cdot\text{L}^{-1})$ ,  $r = 0.996$ , for cadmium and lead, respectively. The limits of detection were 4.2  $\mu\text{M}$  and 3.7  $\mu\text{M}$  for cadmium and lead, respectively. The sensitivity (slope of the analytical curve) for the bare flexible copper sensor was higher than for the flexible copper sensor decorated with bismuth micro/nanodendrites for  $\text{Cd}^{2+}$  detection, while for  $\text{Pb}^{2+}$  ions, the highest slope was obtained with the flexible copper sensor decorated with bismuth micro/nanodendrites, demonstrating that the detection system is versatile and able to detect cadmium and lead with either a bare sensor or flexible copper sensor decorated with bismuth micro/nanodendrites. The sensitivity and wider detection range is superior with bismuth micro/nanodendrites due to the ability of bismuth to form alloys with heavy metals, and to its insensitivity to dissolved oxygen [37,38].

Additionally,  $\text{Cd}^{2+}$  and  $\text{Pb}^{2+}$  ions were detected individually in sweat, as illustrated in Figure 4. The current signals at anodic peak potential at  $-0.47\text{ V}$  and  $-0.32\text{ V}$  increased linearly with concentrations in the range of  $2.0 \times 10^{-6}\text{ mol L}^{-1}$  to  $50\text{ }\mu\text{M}$ , as depicted in A for  $\text{Cd}^{2+}$  ions and in C for  $\text{Pb}^{2+}$  ions. The regression line of analytical curve obtained in B for  $\text{Cd}^{2+}$  ions was  $I\text{ (A)} = -4.1 \times 10^{-6} + 1.5 C_{\text{cadmium}}\text{ (mol}\cdot\text{L}^{-1})$ , and the analytical curve obtained in C for  $\text{Pb}^{2+}$  ions was  $-4.03 \times 10^{-5} + 18.8 C_{\text{cadmium}}\text{ (mol}\cdot\text{L}^{-1})$ . The detection limits were 6.6  $\mu\text{M}$  for  $\text{Cd}^{2+}$  ions and 2.6  $\mu\text{M}$  for  $\text{Pb}^{2+}$  ions. The slopes for individual detection were close to those of simultaneous detection, indicating that the flexible copper is versatile and can be used to detect  $\text{Cd}^{2+}$  and  $\text{Pb}^{2+}$  ions simultaneously or individually.

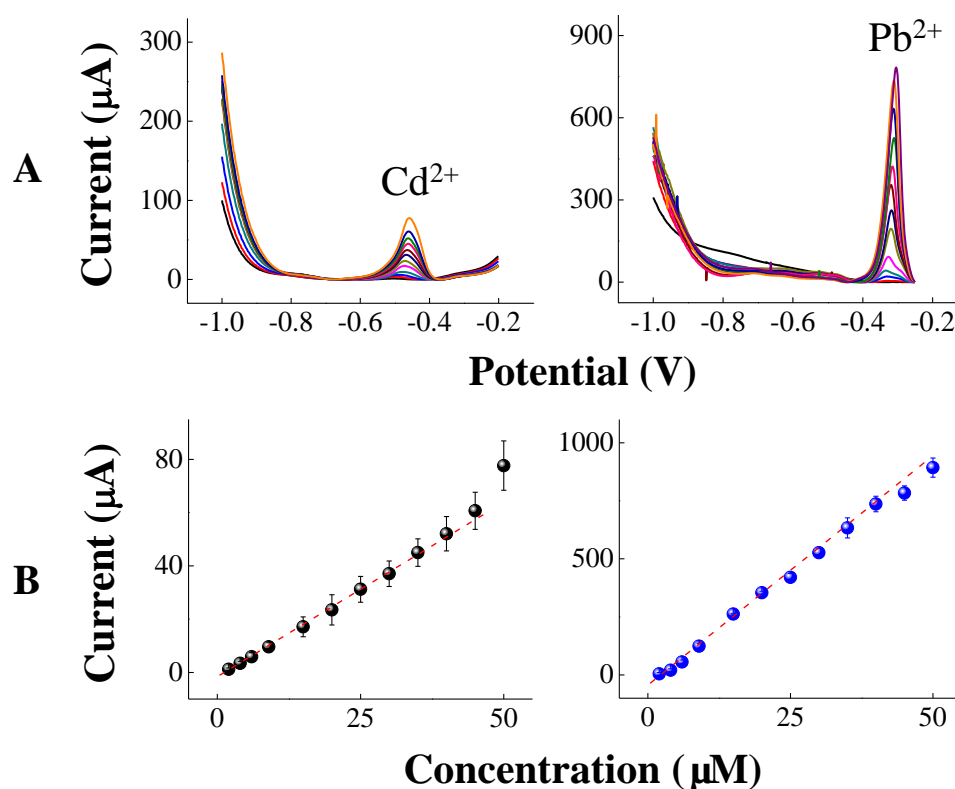


**Figure 4.** Differential pulse anodic stripping voltammetry in (A) and respective analytical curves in (B) for detection of  $\text{Cd}^{2+}$  and  $\text{Pb}^{2+}$  ions using flexible copper sensors decorated with bismuth micro/nanodendrites. Conditions: individual detection of heavy metals with the concentration varying from 2.0  $\mu\text{M}$  to 50  $\mu\text{M}$  in artificial sweat.



The physiological levels of toxic metals in sweat are low ( $<1$  mg/L); in the cases of  $\text{Cd}^{2+}$  and  $\text{Pb}^{2+}$  the concentrations are  $100 \mu\text{g/L}$  [8]. The flexible copper sensor decorated with bismuth micro/nanodendrites was used to determine  $\text{Cd}^{2+}$  and  $\text{Pb}^{2+}$  levels in fortified sweat samples to simulate contaminated sweat. The average recovery ranged from 97.8% to 104.6%. The satisfactory results demonstrate that the flexible copper sensor decorated with bismuth micro/nanodendrites has a high accuracy and potential for  $\text{Cd}^{2+}$  and  $\text{Pb}^{2+}$  sensing in biofluids.

The selectivity of flexible copper sensor decorated with decorated with bismuth micro/nanodendrites was generated with  $2.5 \mu\text{M}$  of glucose, cholesterol, ascorbic acid, dopamine, and uric acid in artificial sweat. Voltammograms obtained for DPASV in Figure 5 indicate a maximum percentage of interference of 10% for dopamine due to a biofouling effect, which could be addressed using a thin layer of Nafion [39]. Copper ions can compete with lead and cadmium for the bismuth active sites on the electrode surface [39]. Zinc ions were not added in the interference study because the oxidation peak is centered between  $-1.4$  V and  $-1.0$  V, leading to strong hydrogen evolution, and  $\text{Zn}^{2+}$  can form chloride complexes with different oxidation states [4,8]. Considering that the flexible device was fabricated with inexpensive flexible copper tape, the results shown in this work are satisfactory; however, they can be enhanced with the use of a high-quality flexible copper tape and a Nafion layer on the bismuth micro/nanodendrites [39].

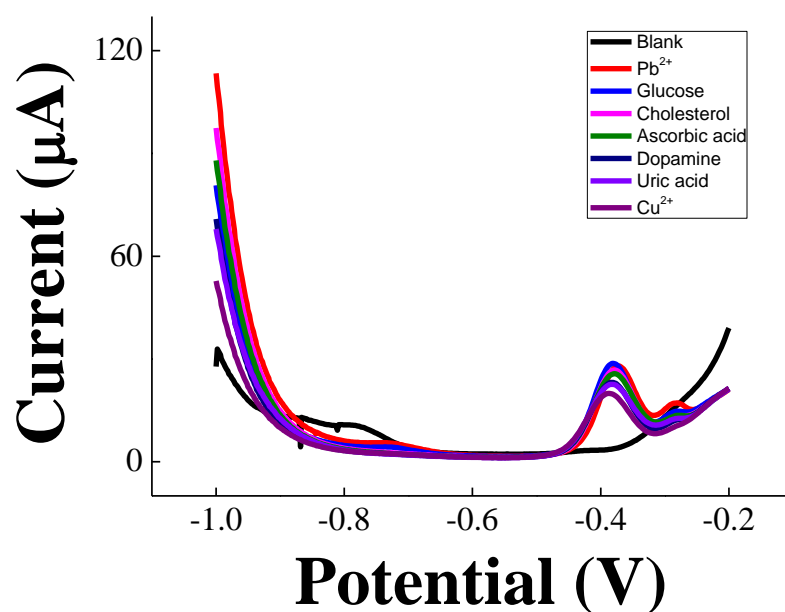


**Figure 5.** Interferent study with glucose, cholesterol, ascorbic acid, dopamine, and uric acid. The concentration for lead and interferents was  $2.5 \mu\text{M}$  in artificial sweat.

Table 1 depicts a list of sensors to detect  $\text{Pb}^{2+}$  and  $\text{Cd}^{2+}$  in different matrices using stripping voltammetry. We could not find any report on the use of flexible copper sensors decorated with bismuth micro/nanodendrites to detect toxic metals (i.e.,  $\text{Pb}^{2+}$  and  $\text{Cd}^{2+}$ ) in sweat. The LOD of this work is higher than in previous studies using different matrices, which may be attributed to the reason that the nature of the copper layer composition is unfavorable when compared to the carbonaceous electrode materials. However, flexible copper sensors decorated with bismuth micro/nanodendrites are highly adaptable to wearable microfluid devices with inexpensive materials. Our method involves simple steps with non-sophisticated materials and an apparatus that can be easily acquired in any local market, such as adhesive label sheets (Pimaco<sup>®</sup>), Silhouette Cameo model 3 cutting machine, and copper adhesive tape. They are cheaper than copper inks, providing an alternative method for copper flexible electrode production to be adapted for microfluidics and wearable devices.

**Table 1.** Figures of merit for Pb<sup>2+</sup> and Cd<sup>2+</sup> ions detection using devices functionalized with bismuth. Due to the limited studies on sensors modified with bismuth micro- nano-structures for determination of Pb<sup>2+</sup> and Cd<sup>2+</sup> ions on relevant biological fluids, figures of merit are also included for environmental purposes.

Modification	Pb <sup>2+</sup>		Cd <sup>2+</sup>		Sample	Ref.
	LOD(μM)	Linear Range (μM)	LOD(μM)	Linear Range (μM)		
Bi/Nafion/Cu	4.3 × 10 <sup>-3</sup>	9.6 × 10 <sup>-3</sup> –0.058	9.8 × 10 <sup>-3</sup>	0.018–0.11	Pb <sup>2+</sup> : ground water Cd <sup>2+</sup> : aquatic plant extracts	[40]
Bi/CuSPE	0.83	1.3–13	0.53	1.0–12	River water	[41]
Bismuth oxide SPE	0.048	0.048–0.72	0.045	0.089–1.3	River water	[42]
BiFME	0.010	0.05–0.35	9.2 × 10 <sup>-3</sup>	0.050–0.35	Mine effluents	[43]
Bi/GCE	9.2 × 10 <sup>-3</sup>	0.024–0.72	0.028	0.044–1.3	Representative pharmaceutical matrices	[44]
Bi <sub>2</sub> O <sub>3</sub> SPCE	9.6 × 10 <sup>-4</sup>	2.4 × 10 <sup>-3</sup> –0.058	1.8 × 10 <sup>-3</sup>	4.4 × 10 <sup>-3</sup> –0.11	Drinking water	[45]
BiNP bulk-modified SPCPE	0.019	8.9 × 10 <sup>-3</sup> –0.44	0.019	4.8 × 10 <sup>-3</sup> –0.24	Urban wastewater	[46]
Bi <sub>nano</sub> /TCE	2.6 × 10 <sup>-3</sup>	0.048–0.24	3.6 × 10 <sup>-3</sup>	0.089–0.44	-	[47]
G/PANI/PS/SPCE	0.016	0.048–2.4	0.039	0.089–4.4	River water	[48]
NC/GCE	1.0 × 10 <sup>-3</sup>	0.010–4.0	-	-	Blueberry extract	[49]
Bi <sub>nanodendrites</sub> /Cu <sub>F</sub>	0.76	2.0–50	5.36	2.0–50	Artificial sweat	This work

Bi/Nafion/Cu, copper electrode modified with Nafion and bismuth; Bi/CuSPE, disposable screen-printed copper electrode modified with bismuth; Bismuth oxide SPE: screen-printed bismuth oxide electrode; Bi/GCE, glassy carbon electrode modified with bismuth; BiFME, carbon-fiber microelectrode modified with Nafion and bismuth; NC/GCE, nitrogen-doped carbon spheres loaded into a glassy carbon electrode; BiNP bulk-modified SPCPE, screen-printed porous carbon electrode modified with Bi nanoparticles; Bi<sub>nano</sub>/TCE, Screen-printed thick-film carbon electrode modified with Bi nanoparticles; G/PANI/PS/SPCE, screen-printed carbon electrode modified with nanoporous fibers, graphene/polyaniline/polystyrene; Bi<sub>nanodendrites</sub>/Cu<sub>F</sub>, flexible copper sensor decorated with bismuth micro/nanodendrites.

#### 4. Conclusions

In this work, we have developed a simple and low-cost method for the design and fabrication of flexible copper sensors through a patterned label on copper adhesive tape, nail polish, and corrosion technique with ferric chloride. The flexible copper sensor with a complete electrochemical system consisted of a pseudo-reference (RE) and working (WE) and auxiliary (AE) electrodes. The working electrode was decorated with bismuth micro/nanodendrites prepared by an easy electrodeposition method on the flexible copper surface. The flexible sensors were used for lead and cadmium detection by DPASV, with a wide linear range between 2.0 μM and 50 μM in artificial sweat samples, high sensitivity of 1.0 A·M<sup>-1</sup> and 6.4 A·M<sup>-1</sup>, and a low limit of detection (LOD) of 5.36 μM and 0.76 μM for Cd<sup>2+</sup> and Pb<sup>2+</sup>, respectively. The determination of toxic metals in artificial sweat showed an easy, fast, inexpensive method for on-site in noninvasive biological samples and environmental analysis.

The advantages of the flexible copper sensor are related to mass production and low cost, and they can be used in organic solvents, e.g., analysis of Pb<sup>2+</sup> and Cd<sup>2+</sup> in fuels, in comparison with screen-printed carbon electrodes. Despite the advances, important challenges remain for the production of flexible copper sensors via an entirely ecofriendly procedure.

In future works, effort is required to design systems using the cutting machine to produce sensors without a corrosion step to avoid waste production and environmental pollution.

**Author Contributions:** A.M.d.C.: Conceptualization, Methodology, Software, Validation, Formal analysis, Investigation, Resources, Writing—Review and Editing. R.R.S.: Resources, Writing—Review and Editing. M.L.C.: Methodology, Investigation, Writing—Review and Editing. P.A.R.-P.: Conceptualization, Methodology, Resources, Writing—Original Draft, Visualization, Writing—Review and Editing, Supervision, Project administration, Funding acquisition. All authors have read and agreed to the published version of the manuscript.

**Funding:** This work was financially supported by Fundação de Amparo à Pesquisa do Estado de São Paulo (FAPESP), Processes number 2016/01919-6, 2022/02164-0 and 2016/06612-6; Conselho Nacional de Desenvolvimento Científico e Tecnológico—CNPq (164569/2020-0, 151200/2022-0, and 423952/2018-8).

**Institutional Review Board Statement:** Not applicable.

**Informed Consent Statement:** Not applicable.

**Data Availability Statement:** Not applicable.

**Acknowledgments:** The authors gratefully acknowledge the financial support granted by the Fundação de Amparo à Pesquisa do Estado de São Paulo (FAPESP), Processes number 2016/01919-6 and 2016/06612-6; Conselho Nacional de Desenvolvimento Científico e Tecnológico—CNPq (164569/2020-0, 151200/2022-0 and 423952/2018-8).

**Conflicts of Interest:** The authors declare no conflict of interest.

## References

1. Anastasova, S.; Crewther, B.; Bembnowicz, P.; Curto, V.; Ip, H.M.; Rosa, B.; Yang, G.-Z. A wearable multisensing patch for continuous sweat monitoring. *Biosens. Bioelectron.* **2017**, *93*, 139–145. [[CrossRef](#)]
2. Bennet, D.; Khorsandian, Y.; Pelusi, J.; Mirabella, A.; Pirrotte, P.; Zenhausern, F. Molecular and physical technologies for monitoring fluid and electrolyte imbalance: A focus on cancer population. *Clin. Transl. Med.* **2021**, *11*, e461. [[CrossRef](#)] [[PubMed](#)]
3. Xu, J.; Fang, Y.; Chen, J. Wearable Biosensors for Non-Invasive Sweat Diagnostics. *Biosensors* **2021**, *11*, 245. [[CrossRef](#)]
4. Xuan, X.; Hui, X.; Yoon, H.; Yoon, S.; Park, J.Y. A rime ice-inspired bismuth-based flexible sensor for zinc ion detection in human perspiration. *Mikrochim. Acta* **2021**, *188*, 97. [[CrossRef](#)] [[PubMed](#)]
5. Bandodkar, A.J.; Jia, W.; Wang, J. Tattoo-Based Wearable Electrochemical Devices: A Review. *Electroanalysis* **2015**, *27*, 562–572. [[CrossRef](#)]
6. Qiao, L.; Benzigar, M.R.; Subramony, J.A.; Lovell, N.H.; Liu, G. Advances in Sweat Wearables: Sample Extraction, Real-Time Biosensing, and Flexible Platforms. *ACS Appl. Mater. Interfaces* **2020**, *12*, 34337–34361. [[CrossRef](#)]
7. Ray, T.R.; Choi, J.; Bandodkar, A.J.; Krishnan, S.; Gutruf, P.; Tian, L.; Ghaffari, R.; Rogers, J.A. Bio-Integrated Wearable Systems: A Comprehensive Review. *Chem. Rev.* **2019**, *119*, 5461–5533. [[CrossRef](#)]
8. Gao, W.; Nyein, H.Y.Y.; Shahpar, Z.; Fahad, H.M.; Chen, K.; Emaminejad, S.; Gao, Y.; Tai, L.-C.; Ota, H.; Wu, E.; et al. Wearable Microsensor Array for Multiplexed Heavy Metal Monitoring of Body Fluids. *ACS Sens.* **2016**, *1*, 866–874. [[CrossRef](#)]
9. Ferreira-Ceccato, A.D.; Ramos, E.M.C.; de Carvalho, L.C.S.; Xavier, R.F.; Teixeira, M.F.D.S.; Raymundo-Pereira, P.A.; Proença, C.D.A.; de Toledo, A.C.; Ramos, D. Short terms effects of air pollution from biomass burning in mucociliary clearance of Brazilian sugarcane cutters. *Respir. Med.* **2011**, *105*, 1766–1768. [[CrossRef](#)]
10. Landrigan, P.J.; Lucchini, R.; Kotelchuck, D.; Grandjean, P. Principles for Prevention of the Toxic Effects of Metals. In *Handbook on the Toxicology of Metals*, 4th ed.; Academic Press: Cambridge, MA, USA, 2015; pp. 507–528. [[CrossRef](#)]
11. Wani, A.L.; Ara, A.; Usmani, J.A. Lead toxicity: A review. *Interdiscip. Toxicol.* **2015**, *8*, 55–64. [[CrossRef](#)]
12. Munro, S.; Ebdon, L.; McWeeny, D.J. Application of inductively coupled plasma mass spectrometry (ICP-MS) for trace metal determination in foods. *J. Anal. At. Spectrom.* **1986**, *1*, 211–219. [[CrossRef](#)]
13. Hohnadel, D.C.; Sunderman, F.W.; Nechay, M.W.; McNeely, M.D. Atomic Absorption Spectrometry of Nickel, Copper, Zinc, and Lead in Sweat Collected from Healthy Subjects during Sauna Bathing. *Clin. Chem.* **1973**, *19*, 1288–1292. [[CrossRef](#)]
14. Montiel, V.R.-V.; Sempionatto, J.R.; Vargas, E.; Bailey, E.; May, J.; Bulbarello, A.; Düsterloh, A.; Matusheski, N.; Wang, J. Decentralized vitamin C & D dual biosensor chip: Toward personalized immune system support. *Biosens. Bioelectron.* **2021**, *194*, 113590. [[CrossRef](#)]
15. March, G.; Nguyen, T.D.; Piro, B. Modified Electrodes Used for Electrochemical Detection of Metal Ions in Environmental Analysis. *Biosensors* **2015**, *5*, 241–275. [[CrossRef](#)] [[PubMed](#)]

16. Koudelkova, Z.; Syrový, T.; Ambrozová, P.; Moravec, Z.; Kubac, L.; Hýnek, D.; Richtera, L.; Adam, V. Determination of Zinc, Cadmium, Lead, Copper and Silver Using a Carbon Paste Electrode and a Screen Printed Electrode Modified with Chromium(III) Oxide. *Sensors* **2017**, *17*, 1832. [[CrossRef](#)]
17. Lee, S.; Park, S.-K.; Choi, E.; Piao, Y. Voltammetric determination of trace heavy metals using an electrochemically deposited graphene/bismuth nanocomposite film-modified glassy carbon electrode. *J. Electroanal. Chem.* **2016**, *766*, 120–127. [[CrossRef](#)]
18. Hassan, K.M.; Gaber, S.E.; Altahan, M.F.; Azzem, M.A. Single and simultaneous voltammetric sensing of lead(II), cadmium(II) and zinc(II) using a bimetallic Hg-Bi supported on poly(1,2-diaminoanthraquinone)/glassy carbon modified electrode. *Sens. Bio-Sensing Res.* **2020**, *29*, 100369. [[CrossRef](#)]
19. Peshoria, S.; Narula, A.K. Bare indium tin oxide electrode for electrochemical sensing of toxic metal ion. *J. Mater. Sci. Mater. Electron.* **2018**, *29*, 13858–13863. [[CrossRef](#)]
20. Bohari, N.A.; Siddiquee, S.; Saallah, S.; Misson, M.; Arshad, S.E. Optimization and Analytical Behavior of Electrochemical Sensors Based on the Modification of Indium Tin Oxide (ITO) Using PANI/MWCNTs/AuNPs for Mercury Detection. *Sensors* **2020**, *20*, 6502. [[CrossRef](#)] [[PubMed](#)]
21. Khoshroo, A.; Sadrijavadi, K.; Taran, M.; Fattahi, A. Electrochemical system designed on a copper tape platform as a nonenzymatic glucose sensor. *Sensors Actuators B Chem.* **2020**, *325*, 128778. [[CrossRef](#)]
22. Soares, J.C.; Soares, A.C.; Rodrigues, V.C.; Oiticica, P.R.A.; Raymundo-Pereira, P.A.; Bott-Neto, J.L.; Buscaglia, L.A.; de Castro, L.D.C.; Ribas, L.C.; Scabini, L.; et al. Detection of a SARS-CoV-2 sequence with genosensors using data analysis based on information visualization and machine learning techniques. *Mater. Chem. Front.* **2021**, *5*, 5658–5670. [[CrossRef](#)]
23. Raymundo-Pereira, P.A.; Shimizu, F.M.; Coelho, D.; Piazzeta, M.H.; Gobbi, A.L.; Machado, S.A.; Oliveira, O.N. A Nanostructured Bifunctional platform for Sensing of Glucose Biomarker in Artificial Saliva: Synergy in hybrid Pt/Au surfaces. *Biosens. Bioelectron.* **2016**, *86*, 369–376. [[CrossRef](#)]
24. Nasraoui, S.; Ameer, S.; Al-Hamry, A.; Ben Ali, M.; Kanoun, O. Development of an Efficient Voltammetric Sensor for the Monitoring of 4-Aminophenol Based on Flexible Laser Induced Graphene Electrodes Modified with MWCNT-PANI. *Sensors* **2022**, *22*, 833. [[CrossRef](#)] [[PubMed](#)]
25. Yu, W.W.; White, I.M. Inkjet-printed paper-based SERS dipsticks and swabs for trace chemical detection. *Analyst* **2012**, *138*, 1020–1025. [[CrossRef](#)]
26. Mannoor, M.S.; Tao, H.; Clayton, J.D.; Sengupta, A.; Kaplan, D.L.; Naik, R.R.; Verma, N.; Omenetto, F.G.; McAlpine, M. Graphene-based wireless bacteria detection on tooth enamel. *Nat. Commun.* **2012**, *3*, 763. [[CrossRef](#)]
27. Scordo, G.; Moscone, D.; Pallechi, G.; Arduini, F. A reagent-free paper-based sensor embedded in a 3D printing device for cholinesterase activity measurement in serum. *Sensors Actuators B Chem.* **2018**, *258*, 1015–1021. [[CrossRef](#)]
28. Honda, W.; Harada, S.; Arie, T.; Akita, S.; Takei, K. Wearable, Human-Interactive, Health-Monitoring, Wireless Devices Fabricated by Macroscale Printing Techniques. *Adv. Funct. Mater.* **2014**, *24*, 3299–3304. [[CrossRef](#)]
29. Li, X.; Tian, J.; Nguyen, T.; Shen, W. Paper-Based Microfluidic Devices by Plasma Treatment. *Anal. Chem.* **2008**, *80*, 9131–9134. [[CrossRef](#)] [[PubMed](#)]
30. Brazaca, L.C.; Imamura, A.H.; Gomes, N.O.; Almeida, M.B.; Scheidt, D.T.; Raymundo-Pereira, P.A.; Oliveira, O.N.; Janegitz, B.C.; Machado, S.A.S.; Carrilho, E. Electrochemical immunosensors using electrodeposited gold nanostructures for detecting the S proteins from SARS-CoV and SARS-CoV-2. *Anal. Bioanal. Chem.* **2022**, *414*, 5507–5517. [[CrossRef](#)] [[PubMed](#)]
31. Wang, J. Stripping Analysis at Bismuth Electrodes: A Review. *Electroanalysis* **2005**, *17*, 1341–1346. [[CrossRef](#)]
32. Mathew, M.; Ariza, E.; Rocha, L.; Fernandes, A.; Vaz, F. TiCxOy thin films for decorative applications: Tribocorrosion mechanisms and synergism. *Tribol. Int.* **2008**, *41*, 603–615. [[CrossRef](#)]
33. de Figueiredo-Filho, L.C.; Baccarin, M.; Janegitz, B.C.; Fatibello-Filho, O. A disposable and inexpensive bismuth film minisensor for a voltammetric determination of diquat and paraquat pesticides in natural water samples. *Sensors Actuators B Chem.* **2017**, *240*, 749–756. [[CrossRef](#)]
34. Salazar-Pérez, A.J.; Camacho-López, M.; Morales-Luckie, R.A.; Sánchez-Mendieta, V. Structural evolution of Bi<sub>2</sub>O<sub>3</sub> prepared by thermal oxidation of bismuth nanoparticles. *Soc. Mex. Cienc. Tecnol. Superf. Mater.* **2005**, *18*, 4–8.
35. Meng, L.; Xu, W.; Zhang, Q.; Yang, T.; Shi, S. Study of nanostructural bismuth oxide films prepared by radio frequency reactive magnetron sputtering. *Appl. Surf. Sci.* **2019**, *472*, 165–171. [[CrossRef](#)]
36. Zhong, H.; Qiu, Y.; Zhang, T.; Li, X.; Zhang, H.; Chen, X. Bismuth nanodendrites as a high performance electrocatalyst for selective conversion of CO<sub>2</sub> to formate. *J. Mater. Chem. A* **2016**, *4*, 13746–13753. [[CrossRef](#)]
37. Torma, F.; Kádár, M.; Tóth, K.; Tatár, E. Nafion®/2,2'-bipyridyl-modified bismuth film electrode for anodic stripping voltammetry. *Anal. Chim. Acta* **2008**, *619*, 173–182. [[CrossRef](#)]
38. Chaiyoi, S.; Apiluk, A.; Siangproh, W.; Chailapakul, O. High sensitivity and specificity simultaneous determination of lead, cadmium and copper using  $\mu$ PAD with dual electrochemical and colorimetric detection. *Sensors Actuators B Chem.* **2016**, *233*, 540–549. [[CrossRef](#)]
39. Zhao, G.; Liu, G. Synthesis of a three-dimensional (BiO)<sub>2</sub>CO<sub>3</sub>@single-walled carbon nanotube nanocomposite and its application for ultrasensitive detection of trace Pb(II) and Cd(II) by incorporating Nafion. *Sensors Actuators B Chem.* **2019**, *288*, 71–79. [[CrossRef](#)]
40. Legeai, S.; Vittori, O. A Cu/Nafion/Bi electrode for on-site monitoring of trace heavy metals in natural waters using anodic stripping voltammetry: An alternative to mercury-based electrodes. *Anal. Chim. Acta* **2006**, *560*, 184–190. [[CrossRef](#)]

41. Figueiredo-Filho, L.C.S.; Janegitz, B.C.; Fatibelilo-Filho, O.; Marcolino-Junior, L.H.; Banks, C.E. Inexpensive and disposable copper mini-sensor modified with bismuth for lead and cadmium determination using square-wave anodic stripping voltammetry. *Anal. Methods* **2012**, *5*, 202–207. [[CrossRef](#)]
42. Kadara, R.O.; Jenkinson, N.; Banks, C.E. Disposable Bismuth Oxide Screen Printed Electrodes for the High Throughput Screening of Heavy Metals. *Electroanalysis* **2009**, *21*, 2410–2414. [[CrossRef](#)]
43. Peña, R.C.; Cornejo, L.; Bertotti, M.; Brett, C.M.A. Electrochemical determination of Cd(ii) and Pb(ii) in mining effluents using a bismuth-coated carbon fiber microelectrode. *Anal. Methods* **2018**, *10*, 3624–3630. [[CrossRef](#)]
44. Rosolina, S.M.; Chambers, J.Q.; Lee, C.W.; Xue, Z.-L. Direct determination of cadmium and lead in pharmaceutical ingredients using anodic stripping voltammetry in aqueous and DMSO/water solutions. *Anal. Chim. Acta* **2015**, *893*, 25–33. [[CrossRef](#)]
45. Riman, D.; Jirovsky, D.; Hrbac, J.; Prodromidis, M.I. Green and facile electrode modification by spark discharge: Bismuth oxide-screen printed electrodes for the screening of ultra-trace Cd(II) and Pb(II). *Electrochem. Commun.* **2015**, *50*, 20–23. [[CrossRef](#)]
46. Niu, P.; Fernández-Sánchez, C.; Gich, M.; Navarro-Hernández, C.; Fanjul-Bolado, P.; Roig, A. Screen-printed electrodes made of a bismuth nanoparticle porous carbon nanocomposite applied to the determination of heavy metal ions. *Mikrochim. Acta* **2015**, *183*, 617–623. [[CrossRef](#)]
47. Malakhova, N.A.; Mysik, A.A.; Saraeva, S.Y.; Stozhko, N.; Uimin, M.A.; Ermakov, A.E.; Brainina, K.Z. A voltammetric sensor on the basis of bismuth nanoparticles prepared by the method of gas condensation. *J. Anal. Chem.* **2010**, *65*, 640–647. [[CrossRef](#)]
48. Promphet, N.; Rattanarat, P.; Rangkupan, R.; Chailapakul, O.; Rodthongkum, N. An electrochemical sensor based on graphene/polyaniline/polystyrene nanoporous fibers modified electrode for simultaneous determination of lead and cadmium. *Sensors Actuators B Chem.* **2015**, *207*, 526–534. [[CrossRef](#)]
49. Wu, H.; Qiao, S.; Zhang, N.; Zhang, Y. Preparation of an Electrochemical Sensor for Rapid Detection of Lead(II) in Blueberries. *Int. J. Electrochem. Sci.* **2021**, *16*, 1–10. [[CrossRef](#)]